



The morphology and anisotropic growth kinetics of cerium hydride reaction sites



John P. Knowles^{a,*}, Georgia Rule^{a,b}, Martin Brierley^a

^a AWE plc, Aldermaston, Reading, Berkshire RG7 4PR, United Kingdom

^b University of Nottingham, School of Chemistry, Nottingham, Nottinghamshire NG7 2RD, United Kingdom

ARTICLE INFO

Article history:

Received 28 February 2013

Accepted 13 July 2013

Available online 20 July 2013

Keywords:

A. Rare earth elements

C. Kinetic parameters

C. Pitting corrosion

ABSTRACT

The lateral and penetrative growth velocities of cerium hydride reaction sites under 100 mbar of hydrogen at 30 °C have been determined from a combination of *in situ* imaging and post reaction optical and electron microscopy. Scanning electron microscopy resolved small hydride sites (<100 μm) in the initial stages of growth and ion-etching revealed these sites to be comprised of a poly-crystalline core surrounded by a corona of deformed material. Extended-focus optical microscopy revealed larger reaction sites (>100 μm) had grown with oblate hemispherical morphology as a consequence of anisotropic growth kinetics.

Crown Copyright © 2013 Published by Elsevier Ltd. All rights reserved.

1. Introduction

Various metals have the potential to form hydride phases [1]. During extended periods of storage, environmental conditions can develop that enable the hydride phase to form. The formation of hydride phases has safety implications such as the potential to adversely change mechanical properties [2] and to cause unintended thermal excursions, pressurisations and/or breaches of containment [3–5]. To underwrite long-term storage, a predictive model of hydriding behaviour is desirable and requires detailed understanding. Investigating the growth kinetics and morphologies of metal hydride reaction sites is of fundamental importance to model development. Using cerium as an example of a hydride forming metal, this paper details a post-experimental analysis developed to investigate the morphology and growth kinetics of the hydride phase.

It is well established that cerium reacts exothermically with hydrogen to form a hydride phase [6]. Upon reaction the CeH₂ phase is formed although additional hydrogen can be accommodated as a heterogeneous solid solution of non-stoichiometric hydrides CeH_{2+x} (0 < x < 1) up to CeH₃ [7,8]. Initially cerium will react with hydrogen in a localised manner forming discrete hydride sites [9]. Provided adequate time and hydrogen, the reaction sites will continue growing and eventually coalesce into a coherent reaction front [10].

Much is known concerning the bulk properties of cerium hydride [11], the hydrogen reactivity of cerium surfaces [12,13] and

formation rates of cerium hydride [9,10,14]. The growth velocity of cerium hydride is generally discussed in terms of a moving reaction front. Individual reaction site growth kinetics are quantified in terms of a boundary displacement velocity (lateral growth) of the reaction sites across the surface [9]. Bulk reaction velocities are defined by the penetration velocity of a coherent reaction front into the bulk metal [1].

An inconsistency in the hydriding kinetics of cerium between the bulk hydriding velocity (V_b) [14] and lateral growth velocities of individual reactions sites (V_l) [9] has been observed. It has been suggested that the morphology of reaction sites correlates with the inconsistency between the velocities of the reacting front i.e. V_b and V_l ; assuming V_b is identical to the penetrative velocity (V_p) of an individual reaction site [1]. However, a correlation between the morphology of a reaction site with anisotropic growth kinetics has not been established experimentally. Therefore, using a combination of *in situ* visual analysis and post experimental microscopy, this study has investigated the relationships between the morphology of discrete reaction sites and the kinetics parameters V_b , V_l and V_p .

2. Materials and methods

A cylindrical sample of cerium (12 mm diameter, 2 mm thick) was machined from a cast rod (99.9% purity, Goodfellow) using a Buehler Isomet 5000 linear precision saw. Ultra pure hydrogen (>99.99998%) was generated using a Parker Balston hydrogen generator and further purified by storage over LaNi₅. A typical metallographic image is shown in Fig. 1. The cerium was found to consist of well-defined grains with sizes between 10–30 μm. X-ray diffraction demonstrated the material to be single phase γ-cerium.

* Corresponding author. Tel.: +44 01189851610.

E-mail address: john.knowles@awe.co.uk (J.P. Knowles).

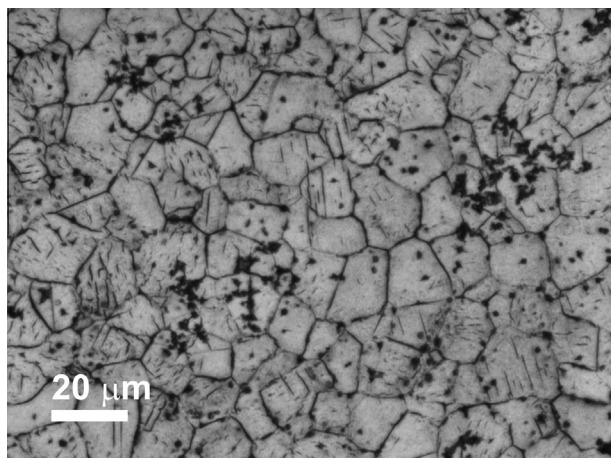


Fig. 1. Metallographic image (20 μm scale bar).

2.1. Hydriding experiment

The experiment was performed using a stainless steel reaction vessel with an integrated viewing window. Pumping and gas supply was provided by a gas handling line capable of attaining a base pressure of 10^{-7} mbar. The sample was wet abraded using ethanol as a lubricant on SiC paper to remove the gross oxide layer. The sample was exposed to air for exactly 20 min and then evacuated for 18 h at 30 °C. The reaction was conducted at 30 °C under a hydrogen pressure of 0.1 bar. A CCD camera recorded images of the visible reacting surface every second during the course of the reaction. Type K thermocouples and MKS mini-Baratrons™ were used to monitor temperatures and pressures. Readings were recorded periodically throughout the experiment using Orchestra™ software. Following reaction, the sample was passivated by a short exposure to oxygen. The sealed reaction vessel was transferred to an argon filled glove box where removal of adherent reaction product was achieved by wiping with soft cotton buds. The cleaned sample was removed from the glove box and stored under oil ready for analysis.

2.2. Extended-focus microscopy

Extended-focus three dimensional imaging of hydride sites was performed using a Zeiss Axio Imager M1 m microscope under ambient laboratory conditions. Three-dimensional representations were calibrated in the x,y plane against a Psyer-SG1 calibration stick with graduations of 0.1 mm and the z direction by means of a calibrated stepper motor. Prior to imaging, the sample was extensively sonicated in ethanol, which degreased the sample and removed any residual hydride still adhered within the sites.

2.3. Scanning electron microscopy

Secondary electron images were obtained using a JEOL FEG-SEM JSM7000F operated at 15 keV and a chamber vacuum of 10^{-4} Pa. Images were collected before and after argon ion etching in a Gatan Model 682 PECS™ operated with a chamber vacuum of 10^{-3} Pa, at 300 μA and an acceleration voltage of 8.6 kV for 173 min. Sample transfers between instruments were conducted under ambient laboratory conditions lasting *ca* 30 s.

2.4. Vickers hardness indentation

An additional sample was prepared specifically for hardness measurements. The sample was prepared as described above but

was left to react with hydrogen until the hydride reactions sites had grown to macroscopic sizes (>1 mm diameter). This sample was not passivated or cleaned but removed from the cell and set in epoxy resin. Cross sectioning, grinding and polishing was conducted to reveal a section through a hydride crater containing a 200 μm thick layer of adherent hydride. The hardness of the hydride and metal phases were measured in triplicate using a Leco V-100-A2 Vickers hardness indenter with a 1 kg load.

3. Results and discussion

3.1. Nucleation and growth

Monitoring the reacting surface using *in situ* imaging enabled the nucleation and growth kinetics of cerium hydride sites to be determined. Fig. 2 depicts the number of sites observed and the consumption of hydrogen as a function of reaction time. The reaction was stopped before any corrosion sites had converged by evacuating the hydrogen; in total, 19 discrete reaction sites were observed. The nucleation behaviour is typical of that expected for a reactive metal undergoing a diffusion barrier controlled nucleation process where the oxide over-layer acts as the barrier [15,16]. A clear correlation between the consumption of hydrogen and the nucleation rate is evident.

The growth of individual reaction sites was also monitored as a function of time from the *in situ* imaging. Plots depicting the variation in reaction site radii as a function of time for the six largest reaction sites are shown in Fig. 3. The radial growth of the reaction

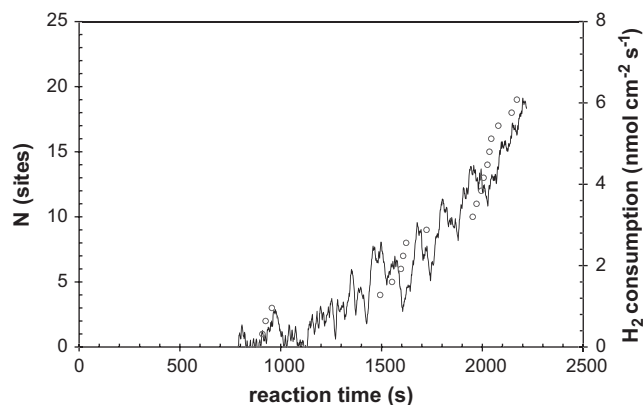


Fig. 2. The nucleation of hydride sites ($N \circ$) and the consumption of hydrogen (—) as a function of reaction time.

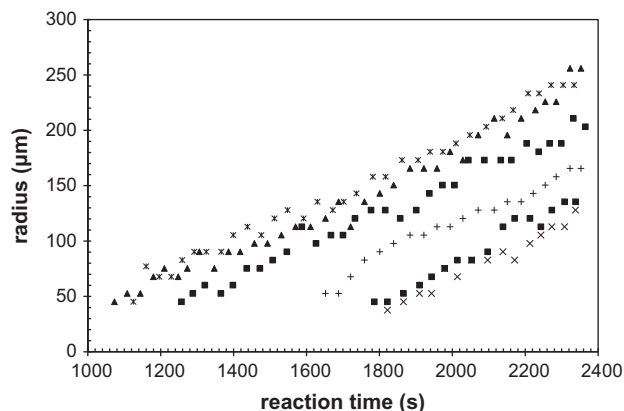


Fig. 3. The growth in the lateral radii as a function of reaction time for six reaction sites.

Download English Version:

<https://daneshyari.com/en/article/7896099>

Download Persian Version:

<https://daneshyari.com/article/7896099>

[Daneshyari.com](https://daneshyari.com)